water

MDPI

Article

An Assessment of Trends of Potential Evapotranspiration at Multiple Timescales and Locations in Sicily from 2002 to 2022

Tagele Mossie Aschale [1,2], Nunziarita Palazzolo [1], David J. Peres [1,*], Guido Sciuto [3] and Antonino Cancelliere [1]

1 Department of Civil Engineering and Architecture, University of Catania, Via A. Doria 6, 95125 Catania, Italy
2 Department of Geography and Environmental Studies, Debre Markos University, Debre Markos P.O. Box 269, Ethiopia
3 Ambiens Srl, Via Roma, 44, 94019 Valguarnera Caropepe, Italy
* Correspondence: djperes@dica.unict.it

Abstract: Climate change and the related temperature rise can cause an increase in evapotranspiration. Thus, the assessment of potential evapotranspiration (PET) trends is important to identify possible ongoing signals of climate change, in order to develop adaptation measures for water resource management and improve irrigation efficiency. In this study, we capitalize on the data available from a network of 46 complete meteorological stations in Sicily that cover a period of about 21 years (2002–2022) to estimate PET by the Food and Agriculture Organization (FAO) using the Penman –Monteith method at the daily time scale in Sicily (southern Italy). We then analyse the trends of PET and assess their significance by Sen's Slope and the Mann–Kendall test at multiple temporal scales (monthly, seasonal, and annual). Most of the locations do not show significant trends. For instance, at the annual timescale, only five locations have a significantly increasing trend. However, there are many locations where the monthly trend is statistically significant. The number of locations where monthly trend is significant is maximum for August, where 18 out of these 46 stations have an increasing trend. In contrast, in March, there are no locations with a significant trend. The location with the highest increasing trend of PET indicates trend slopes of 1.73, 3.42, and 10.68 mm/year at monthly (August), seasonal (summer), and annual timescales, respectively. In contrast, decreasing PET trends are present only at the monthly and seasonal scales, with a maximum of, respectively, −1.82 (July) and −3.28 (summer) mm/year. Overall, the findings of this study are useful for climate change adaptation strategies to be pursued in the region.

Keywords: climate change; temperature; drought; irrigation; Mediterranean area; Penman-Monteith

check for updates

Citation: Aschale, T.M.; Palazzolo, N.; Peres, D.J.; Sciuto, G.; Cancelliere, A. An Assessment of Trends of Potential Evapotranspiration at Multiple Timescales and Locations in Sicily from 2002 to 2022. *Water* **2023**, *15*, 1273. https://doi.org/10.3390/w15071273

Academic Editor: Aizhong Ye

Received: 28 February 2023
Revised: 10 March 2023
Accepted: 14 March 2023
Published: 23 March 2023

1. Introduction

Global warming induced by greenhouse gas emissions is claimed to be a key contributor to changes in the global climate [1–3]. The Fifth Assessment Report (AR5) by the IPCC discusses how the last three decades have been successively warmer at the Earth's surface than any preceding decade since 1850. Global warming is claimed to influence the entire hydrological cycle [4–7]. Assessments of potential evapotranspiration (PET) show that evapotranspiration can be considerably influenced by global climatic changes [5,8–10]. The IPCC's sixth technical report showed that there is an increase in evapotranspiration due to growing atmospheric water demand which will decrease soil moisture in the Mediterranean region [1].

Evapotranspiration is also a key variable for the estimation of the energy budget in the Earth's atmospheric system and the water balance in a given region [5,10–12]. PET refers to evaporation and transpiration over a surface under certain meteorological conditions considering sufficient water and an unlimited soil water supply. Moreover, PET is important for scientific research on hydro-climatology, irrigation planning, and water resource management [4,6,8].

Understanding the spatiotemporal trends of PET is a crucial part of climatology, water resource management, and irrigation planning [13]. Both decreasing and increasing trends of PET have been detected in different parts of the world [7,14–18]. PET is expected to increase due to climate change. Nevertheless, decreasing trends have been identified, leading to the so-called "evapotranspiration paradox" [4,8,18–20], and it was detected in several regions worldwide, especially in various areas of China [7,8,10–12,16]. For the Mediterranean climate, [21] showed that 14 studies confirmed prevailing positive trends, 4 studies negative trends, and 3 studies no trends. From 1961 to 2016, the trend of the reference evapotranspiration from 18 meteorological stations in Slovenia was analysed and the result showed that samples are mostly increasing and statistically significant while no consistent trend could be detected [22]. In the western French Mediterranean area, the PET showed an increasing trend at the monthly, seasonal (spring), and annual scales from 1970 to 2006 [23].

The Mediterranean area also showed there was an increasing trend of PET from 1950 to 2020 which significantly contributed to drought intensification in the region [24]. The actual evapotranspiration also showed a trend in the humid and subhumid Mediterranean climate of North Algeria from 1961 to 1990 [25]. Moreover, for the Mediterranean, future projections of PET also confirmed that there will be an increasing trend [26]. Additionally, in Greece, the PET showed an increasing trend [27]; in southern Italy, it showed an increasing trend in the growing season [28]. According to Liuzzo et al. (2016), there were seasonal differences in the spatiotemporal trend of PET in different areas of Mediterranean climate. For instance, in southern Italy, an increasing trend was observed in correspondence with the growing season, whereas no trend was observed during the non-growing season. However, the mentioned study needs to be updated as it considers an outdated period and only three locations in Sicily.

In this study, we advance from previous studies by considering a dataset that covers a recent period (last 21 years, up to 2022) and 46 locations spread in Sicily. This allows an unprecedented systematic and robust assessment of the PET trend in this region, which is prone to droughts and presents several critical factors in relation to climate change [29]. In particular, in the present study, we analyse the PET trends in Sicily at multiple locations (i.e., those of meteorological stations managed by the SIAS-Servizio Informativo Agrometeorologico Siciliano-the Agrometeorological Informative Service of Sicily) at the monthly, seasonal, and annual temporal scales.

This paper is organized as follows. After this introduction, the study area and the data are described, and the methodology is delineated (Section 2). This section explains the methods for computing PET and the statistical methods for assessing the magnitude and significance of trends. Then, in Section 3, the results are presented, analysing various time scales. Section 4 discusses the results with a comparison to other regions on the globe. Finally, Section 5 presents some conclusions and an outlook.

2. Material and Methods

2.1. Study Area and Data

Figure 1 shows the study area, Sicily. The climate of Sicily is typically Mediterranean, with hot but not scorching summers, mild and brief winters, and moderate rainfall from October to March. Along the coast, the average temperature ranges between 17 and 18.7 °C annually, with July being the warmest month [30]. Sicily's weather is characterized by a hot and dry summer season, and a mild and rainy winter season [31]. The meteorological data are provided by the Agrometeorological Information Service of Sicily (SIAS, http://www.sias.regione.sicilia.it/ accessed on 16 March 2023), which has 46 meteorological stations distributed all over the region. Specifically, for each meteorological station, minimum, maximum, and mean temperature (°C), solar radiation (MJ/m^2), wind speed (m/s), and relative humidity (%) are collected from 1 January 2002 to 31 March 2022. Table 1 summarizes the main characteristics of each station, namely, name, ID, elevation, and the coordinates of their location.

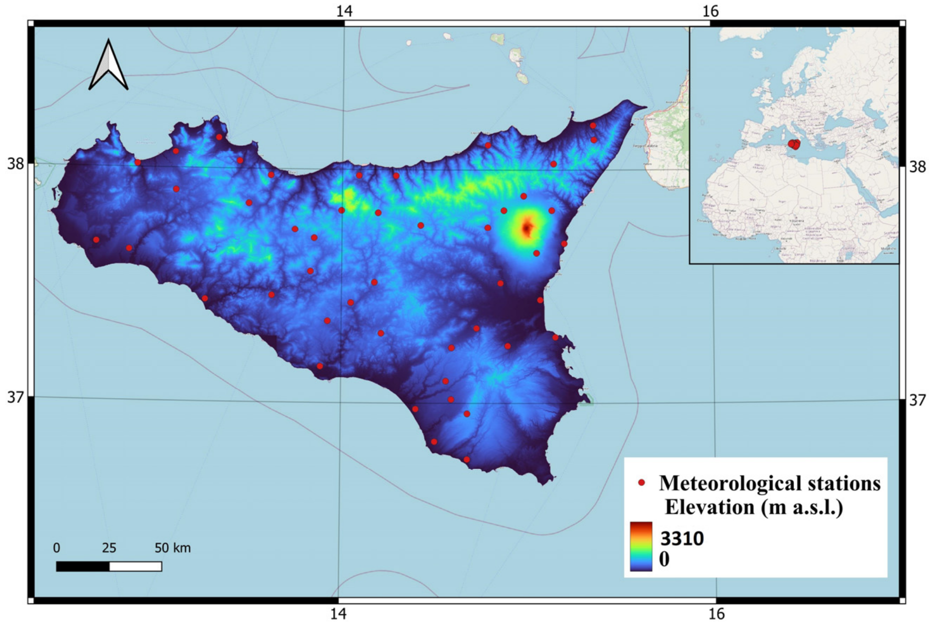

Figure 1. Study area with location of meteorological stations of the SIAS network.

Table 1. Main characteristics of the SIAS network meteorological stations.

Code	Name	Elevation [m a.s.l.]	Annual Average PET [mm]
203	Aragona	305	1091.19
209	Licata	80	1368.18
212	Ribera	30	1119.13
214	Caltanissetta	350	1175.23
215	Delia	360	1138.6
218	Mazzarino	480	1107.06
219	Mussomeli	650	1189.08
224	Bronte	430	1040.83
227	Caltagirone	480	1101.61
228	Catania	10	1200.8
229	Riposto	50	1079.57
230	Linguaglossa	590	1049.76
231	Maletto	1040	1032.93
232	Mazzarrone	300	1177.1
233	Mineo	200	1084.08
234	Paternò	100	1156.05
235	Pedara	810	1015.08
237	Randazzo	680	1128.66
238	Enna	350	1176.78
241	Nicosia	700	1024.62
249	S. Pier Niceto	460	1103.05
254	Naso	480	948.26
256	Novara di Sicilia	750	1045.11
258	Pettineo	210	1160.26
261	Torregrotta	60	1098.13
262	Alia	560	1163.41
264	Camporeale	460	1090.79
265	Castelbuono	430	1158.36
269	Gangi	830	1105.08
273	Mezzojuso	390	1084.26
274	Misilmeri	160	1070.78
276	Palermo	50	1087.91
277	Partinico	120	1055.93

Table 1. *Cont.*

Code	Name	Elevation [m a.s.l.]	Annual Average PET [mm]
279	Polizzi Generosa	650	1106.09
222	Sclafani Bagni	497	1066.29
281	Termini Imerese	350	1086.66
282	Acate	60	1100.15
283	Comiso	220	1099.55
286	Ragusa	650	1163.68
287	Santa Croce Camerina	55	1144.41
288	Scicli	30	1188.86
289	Augusta	60	1074.76
291	Francofonte	100	1220.19
301	Castellammare del Golfo	90	1049.9
302	Castelvetrano	120	1159.07
305	Mazara del Vallo	30	1157.54

2.2. Methodology

The Penman–Monteith method is used in the present study to calculate PET. This method is the most comprehensive and international standard for PET estimation, and it is also approved by the Food and Agriculture Organization (FAO) and the American Society of Civil Engineers (ACSE) [32–37].

The FAO Penman–Monteith equation has been derived by integrating the original Penman–Monteith equation with the equations of the aerodynamic and canopy resistance, yielding the following equation (Equation (1)):

$$\mathrm{PET} = \frac{0.408\Delta(\mathrm{R_n} - \mathrm{G}) + \gamma\frac{\mathrm{C_n}}{\mathrm{T}+273}\mathrm{U_2}(\mathrm{e_s} - \mathrm{e_a})}{\Delta + \gamma(1 + \mathrm{C_d}\,\mathrm{U_2})} \tag{1}$$

where PET is potential evapotranspiration [mm day^{-1}], $\mathrm{R_n}$ is the net radiation at the crop surface [MJ m^{-2} day^{-1}], G represents the soil heat flux density [MJ m^{-2} day^{-1}], T is the air temperature at 2 m height [°C], $\mathrm{U_2}$ represents the wind speed at 2 m height [m s^{-1}], $\mathrm{e_s}$ is the saturation vapour pressure [kPa], $\mathrm{e_a}$ is the actual vapour pressure [kPa], $(\mathrm{e_s} - \mathrm{e_a})$ represents the saturation vapour pressure deficit [kPa], Δ is the slope vapour pressure curve [kPa °C^{-1}], and γ indicates the psychrometric constant [kPa °C^{-1}]. $\mathrm{C_n}$ is the ratio of the slope of the saturation vapour pressure curve to the psychrometric constant at a given temperature. It represents the energy available to drive the process of evapotranspiration. $\mathrm{C_d}$ is the ratio of the aerodynamic resistance to the surface resistance. It represents the resistance that water vapour encounters in the atmosphere as it moves from the leaf surface into the air. In this study, we assume $\mathrm{C_n}$ and $\mathrm{C_d}$ equal 900 and 0.34, which are the values for a grass reference crop.

2.3. Mann–Kendall Test

It is common practice to use the Mann–Kendall (MK) test to identify statistically significant trends in various analyses of hydro-climatological time series [38–44]. It is a rank-based non-parametric method, which has been widely used for detecting trends in hydrometeorological time series. The MK test's key advantage is that it is not sensitive to extreme values and does not require that the data follow any statistical distribution [17,20,45]. The test is based on two hypotheses: the alternative hypothesis ($\mathrm{H_1}$), which shows the existence of a trend and rejects the null hypothesis ($\mathrm{H_0}$), which assumes that the test is stationary and thus there is no trend. Mann–Kendall's statistical S is given by the following formula:

$$\mathrm{S} = \sum_{k=1}^{n-1}\sum_{j=k+1}^{n} \mathrm{Sgn}(\mathrm{X_j} - \mathrm{X_k}) \tag{2}$$

where X_k is the value of the variable at time k, X_j is the value of the variable j, n is the length of the series, and Sgn is a function which is calculated as follows:

$$\mathrm{Sgn}(X_j - X_k) = \begin{cases} 1 \text{ if } (X_j - X_k) > 0 \\ 0 \text{ if } (X_j - X_k) = 0 \\ -1 \text{ if } (X_j - X_k) < 0 \end{cases} \tag{3}$$

It has been documented that, when $n \geq 10$, the statistic S is approximately normally distributed with the mean E(S) = 0, and its variance is:

$$\mathrm{Var}\ (s) = \frac{n(n\ -1)(2n\ +5) - \sum_{i=1}^{m} t_i(t_i - 1)(2t_i + 5)}{18} \tag{4}$$

where n is the number of data points, m is the number of tied groups (a tied group is a set of sample data having the same value), and t_i is the number of data points in the ith group.

The standardized test statistic Z is computed as follows:

$$Z = \begin{cases} \frac{S-1}{\sqrt{\mathrm{Var}(s)}},\ \text{if } S > 0 \\ 0,\ \text{if } S = 0 \\ \frac{S+1}{\sqrt{\mathrm{Var}(s)}},\ \text{if } S < 0 \end{cases} \tag{5}$$

The null hypothesis H_0, meaning that no significant trend is present, is accepted if the test statistic Z is not statistically significant, i.e., $-Z\alpha/2 < Z < Z\alpha/2$, where $Z\alpha/2$ is the standard normal deviation. To overcome the limitation of the MK test related to the autocorrelation of the original data, the trend-free prewhitening (TFPW) method was applied. This method introduced and enabled removing serial dependence, which is one of the main problems in testing and interpreting time series data [46–48].

The trend-free prewhitening includes the following steps:

i. all of the PET time series data were first tested for the presence of an autocorrelation coefficient (r) at a 5% significance level using a two-tailed test.

$$r = \frac{\sum_{t=1}^{n-1} (X_t - \overline{X}_t)(X_{t+1} - \overline{X}_{t+1})}{\sqrt{\sum_{t-1}^{n-1} (X_t - \overline{X}_t)^2} \sqrt{\sum_{t-1}^{n-1} (X_{t+1} - \overline{X}_{t+1})^2}} \tag{6}$$

ii. the autocorrelation coefficient value of r was tested against the null hypothesis at a 95% confidence interval using a two-tailed test

$$r\ (95\%) = \frac{-1 + 1.96\sqrt{(n-2)}}{n-1} \tag{7}$$

iii. removing any trend items from the time series variables to form a sequence without trend items.

$$Y_t = X_t - \beta_t \tag{8}$$

iv. adding the trend term β_t to obtain a new sequence without an autocorrelation effect.

$$Y_t = Y_t - rY_{t-1} + \beta_t \tag{9}$$

where X_t is the value at time t, n is the length of the data, and $\overline{X}_t$ is the mean value. The original MK test is applied to Y_t to assess the significance of the trend.

2.4. Sen's Slope Estimator

Sen's slope estimator is a non-parametric method used for estimating the slope of a linear relationship between two variables [49–53]. It is particularly useful when the data exhibit high variability, non-normal distribution, or outliers. Sen's slope estimator is based on calculating the median of the slopes between all possible pairs of data points. This approach makes it robust to outliers and resistant to extreme values. The method is easy to apply and can be used for small or large datasets. In this study, we used a 0.05 significance level; i.e., when $|Z| > 1.96$ (Equation (5)), the null hypothesis is rejected, and the trend is significant at 5%. If a trend is mentioned in the data series, its amount can be evaluated by the slope of the trend (noted β). In general, this method is used to estimate the slope of the trend [10,54–57]. Hence, the magnitudes of the trends in ETo were studied using Sen's slope estimator.

$$\beta = \text{Median}\left(\frac{X_i - X_j}{i - j}\right) \text{ for all } i > j \quad (10)$$

where X_i and X_j are the data values at times i and j, respectively. $\beta > 0$ denotes an increasing trend.

3. Results

Annual PET trends have been observed only in 5 locations out of 46. Figure 2 shows the PET timeseries for these five locations.

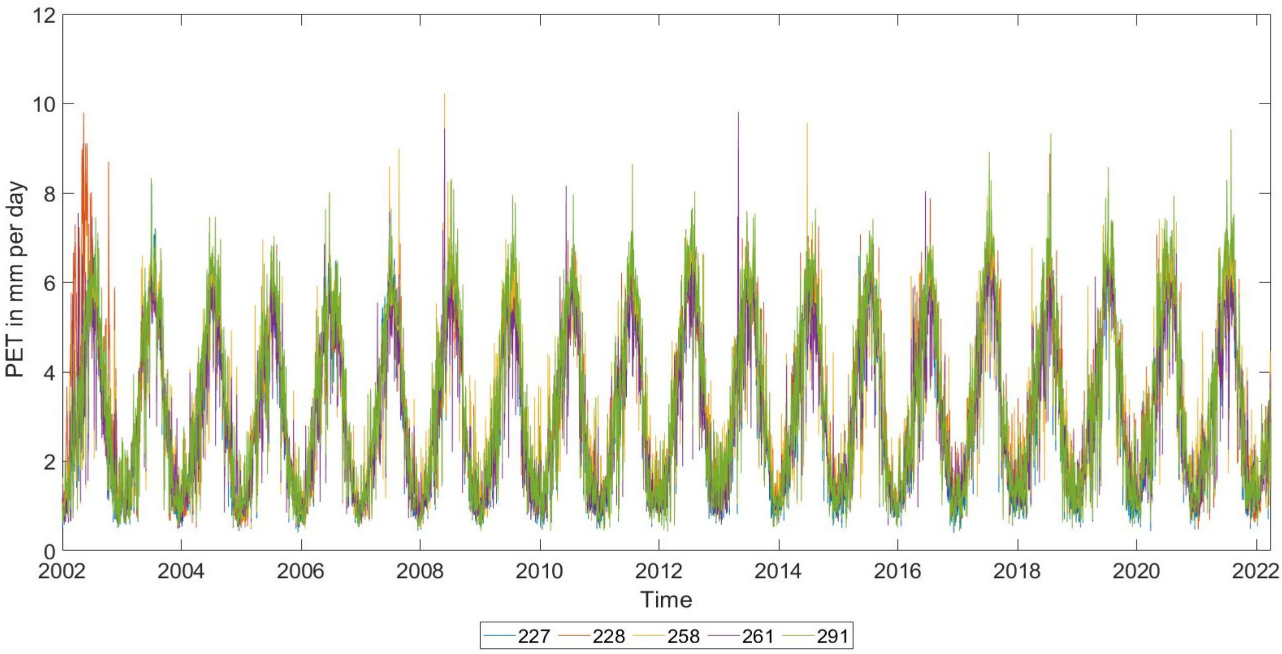

Figure 2. Time series for five meteorological stations confirmed an annual trend.

Table 2 shows that 83% of the meteorological stations recorded a trend in at least one month or season. In terms of PET trend in the last 21 years, 38 out of 46 of the set of analysed meteorological stations resulted in a PET trend at least one temporal scale, whereas only 8 of them do not have any significant trend. Specifically, the latter are mostly located close to the northern and southern coastlines of the island.

Table 2. Z value of the PET trend for each meteorological station at different temporal scales. Yellow shading represents the Z value decreasing PET trend, whereas the reddish shading is the Z value increasing PET trend.

Code	Name	Jan	Feb	Mar	Apr	May	Jun	Jul	Aug	Sep	Oct	Nov	Dec	Win	Spring	Summer	Autumn	Year
203	Aragona	0.68	1.07	−0.23	0.81	−0.42	0	0.68	1.14	1.65	0.55	−0.94	1.01	3.28	0	0.68	1.07	0.94
209	Licata	2.76	1.46	1.27	1.14	0.75	0.29	2.89	3.15	0.49	0.16	0.81	0.84	3.41	0.98	0.81	−0.29	−0.1
212	Ribera	1.27	1.59	0.55	0.94	0.49	2.5	2.82	3.41	2.82	1.72	−1.01	0.03	1.85	0.88	1.82	0.7	0.81
214	Caltanissetta	1.27	1.85	0.81	1.59	0.68	0.03	0.94	0.94	1.33	0.68	−0.55	0.23	0.49	1.26	0.94	0.84	0.62
215	Delia	−0.75	0.55	0.03	0.81	−0.75	−0.52	0.16	1.14	0.91	−0.1	−0.94	0.03	1.05	0.03	0.55	0.1	0.62
218	Mazzarino	2.11	1.78	1.14	1.52	0.62	1.01	1.68	1.65	3.34	1.36	1.52	1.4	0.81	1.59	2.1	2.89	1.85
219	Mussomeli	1.72	1.59	0.94	1.65	0.42	1.14	1.14	2.11	1.91	0.49	−1.01	3.08	1.01	1.14	1.46	0.94	1.91
224	Bronte	2.24	1.69	0.42	2.14	0.88	1.46	1.91	2.08	0.55	1.59	−0.16	1.47	1.27	1.52	2.21	−0.36	0.75
227	Caltagirone	1.52	2.17	0.55	1.65	1.62	0.62	1.72	1.52	1.72	0.36	0.62	2.56	3.28	1.33	1.14	1.14	2.11
228	Catania	−0.42	2.69	1.72	1.72	1.33	1.33	0.62	1.14	0.75	1.07	1.27	1.61	0.94	1.65	1.91	1.98	2.82
229	Riposto	1.27	1.98	0.81	0.42	0.49	0.35	1.52	1.85	1.27	0.49	1.59	0.49	0.36	0.68	1.27	0.84	0.75
230	Linguaglossa	1.14	−0.03	−0.88	0.16	−2.56	−1.52	−0.36	−0.23	0.1	−0.42	−0.23	3.02	1.85	−2.04	−1.4	−0.62	−1.52
231	Maletto	0.55	0.68	−0.81	−0.49	−1.65	−1.98	−2.43	−1.01	−0.29	−1.46	−0.28	0	1.01	−1.2	−2.43	−0.77	−0.42
232	Mazzarrone	1.91	1.27	1.07	0.81	0.42	1.12	0.03	2.17	1.75	1.2	1.07	1.59	2.63	0.55	1.19	0.36	0.42
233	Mineo	0.81	1.07	1.46	0.36	2.11	2.43	2.95	2.24	2.69	1.33	0.49	2.17	2.1	0.81	3.41	0.81	1.52
234	Paternò	1.07	1.2	0.68	0.88	0.42	0.29	−1.12	1.14	2.11	0.88	2.63	0.88	0.55	1.14	1.12	1.98	1.4
235	Pedara	0	−0.03	−0.23	−0.23	−1.52	−1.4	−0.68	−0.03	−0.42	−2.04	−1.01	0.29	1.85	−1.07	−1.65	−2.37	−1.33
237	Randazzo	1.2	0.81	−0.36	−0.55	−1.07	−1.14	−0.36	−0.42	0.36	−1.01	−1.27	0	1.52	−1.01	−0.62	−1.01	−1.07
238	Enna	0.03	1.68	1.27	1.61	1.01	1.33	1.01	2.24	1.68	1.78	0.68	0.62	0.68	0.94	2.3	0.55	0.88
241	Nicosia	1.17	1.85	0.49	2.04	1.07	1.01	1.65	1.33	2.11	0.29	0.58	0.16	0.36	1.72	1.52	1.27	1.01
249	S. P. Niceto	−0.42	−0.16	−0.29	1.07	−0.81	−1.07	−0.49	0.68	1.27	−0.81	−1.72	−1.46	−1.2	−0.55	−0.29	−0.62	−0.68
254	Naso	0	0.36	−1.2	0.88	−1.33	−2.24	−0.81	0.36	−0.32	−0.62	−1.27	−0.49	−0.55	−1.01	−1.07	−1.27	−1.4
256	N. di Sicilia	1.27	1.46	0.23	1.01	−1.07	0.23	1.01	1.59	1.59	−0.68	0.49	0.91	1.27	0.32	1.07	0.23	1.33
258	Pettineo	3.21	2.37	1.2	0.23	0.1	1.07	2.04	2.04	1.65	0.55	0.88	1.59	3.02	1.46	1.98	1.33	3.02
261	Torregrotta	0.62	0.81	1.52	1.3	−0.29	0.42	2.11	2.43	3.08	0.75	0.62	0.75	0.81	1.01	2.37	1.98	3.08
262	Alia	1.17	1.65	1.07	2.04	0.68	0.23	1.01	0.81	0.68	−0.94	−2.56	0.62	1.98	1.14	1.46	−0.81	1.2
264	Camporeale	2.47	1.07	−0.62	0.49	−0.55	−0.84	0.55	1.2	2.11	0.81	−0.75	2.3	1.61	−0.58	0.49	1.43	0.94
265	Castelbuono	2.24	0.62	−1.14	0.49	−0.68	−0.03	1.01	0.75	−0.16	−1.2	−1.14	−0.75	0.88	−0.42	0.75	−1.46	0.03
269	Gangi	1.27	1.72	0.42	1.78	0.62	0.23	1.52	2.08	2.11	−0.03	−0.23	−1.4	1.12	0.68	1.4	−0.16	1.59
273	Mezzojuso	−0.77	−0.1	−1.4	−0.03	−0.58	−1.3	0.55	0.55	−0.16	−1.46	−1.27	−2.11	−1.91	−1.07	−0.62	−2.11	−1.56
274	Misilmeri	1.33	1.78	0.23	1.52	0.03	0.68	2.3	2.04	1.27	0.42	−1.01	0.16	1.07	1.01	1.98	0.16	1.85
276	Palermo	3.19	3.02	1.27	0.42	1.27	0.49	1.91	2.43	0.68	0.49	1.07	0.1	0.36	2.37	2.11	0.29	0.88
277	Partinico	3.47	2.24	0.94	1.59	0.62	1.14	1.82	2.76	2.63	1.07	1.33	1.98	0.81	1.07	2.63	2.5	1.72
279	P. Generosa	0.75	0.88	−0.1	1.52	−0.03	0.75	1.65	1.46	1.14	−0.29	−1.52	−0.16	0.63	0.49	1.33	−0.36	0.75
222	Sclafani Bagni	1.26	2.17	1.01	0.55	1.14	1.27	0.49	2.5	1.47	1.2	0.49	0.62	0.81	1.59	2.43	0.42	1.2
281	Termini Imerese	0.42	1.04	−0.1	0.68	0.16	1.01	2.82	1.78	0.49	−0.81	−1.85	−0.94	0	0.29	2.24	−0.88	0.62
282	Acate	−1.3	−0.68	−0.88	−0.49	−1.52	−0.03	0.81	1.14	0.75	−2.03	−1.59	−1.82	−1.65	−1.59	0.36	−1.59	−1.72
283	Comiso	1.65	1.04	−0.03	0.62	0.94	1.59	3.15	1.98	0.81	0.75	−0.36	1.59	1.65	0.68	2.82	0.03	1.59
286	Ragusa	0.42	0.45	−0.23	0.68	0.55	0.03	0.68	1.2	0.81	−0.94	−1.4	−0.1	1.14	0.03	0.88	−0.16	0.1
287	S. C. Camerina	−2.37	−1.01	−0.94	−0.23	−0.16	1.52	1.85	2.11	0.29	−1.54	−2.11	−2.5	−2.3	−0.88	1.52	−1.2	−1.01
288	Scicli	0.36	−0.23	−0.62	0.16	−0.23	−0.16	0.13	0.29	−0.36	−1.26	−1.46	−0.55	−0.71	−0.23	0.16	−0.94	−0.81
289	Augusta	0.81	0.23	0.55	1.07	−0.23	0.23	0.55	1.4	2.5	−0.62	−0.55	1.12	0.42	0.94	0.36	0.58	0.94
291	Francofonte	1.65	1.59	1.14	1.65	1.4	1.33	0.75	1.78	2.04	0.29	1.52	2.3	2.69	1.91	2.24	1.78	3.08
301	C. del Golfo	1.01	0.55	−1.4	−0.62	−0.23	0.49	1.91	1.07	0.75	−0.16	−2.04	−1.07	0.1	−0.88	1.27	−0.65	−0.16
302	Castelvetrano	2.69	1.52	0.68	0.42	0.62	0.16	2.24	2.5	2.17	1.33	0.42	1.33	0.16	0.49	1.85	−0.49	0.29
305	Mazara del Vallo	0.68	1.2	1.14	0.94	0.36	1.91	0.81	2.76	1.46	1.91	0.62	1.91	0.36	1.27	1.27	1.07	1.4

Table 2, instead, summarizes Z values of the PET trend for each meteorological station and at different temporal scales.

3.1. Temporal Trend of the PET

Looking at the different analysed temporal scales, no increasing trends were observed in March and October. Specifically, in October, exclusively decreasing trends were detected in two meteorological stations, whereas in March, no trend was detected, neither positive nor negative, for all meteorological stations. If an increasing trend of PET is considered, in August and September at a monthly temporal scale, as well as in summer at a seasonal temporal scale, the highest number of involved meteorological stations was recorded, namely, 15 on average for each of these temporal scales. On the contrary, the decreasing trend of PET mostly appeared in November, June, October, and December at a monthly temporal scale and autumn at an annual temporal scale, for each of which the number of the concerned meteorological stations ranges between 2 and 3. Figure 3 provides an overview of the number of meteorological stations displaying or not a trend. As can be seen, for each analysed temporal scale, if mean values are considered with respect to the whole of 46 meteorological stations: (i) about 39 stations do not have a highlighted trend, with a peak in March at the monthly scale with all 46 meteorological stations involved; (ii) about 6 stations recorded an increasing trend of PET, with a peak in August at the monthly scale with 18 stations involved; (iii) only 1 meteorological station recorded a decreasing trend, with a peak equal to 3 in November at the monthly scale.

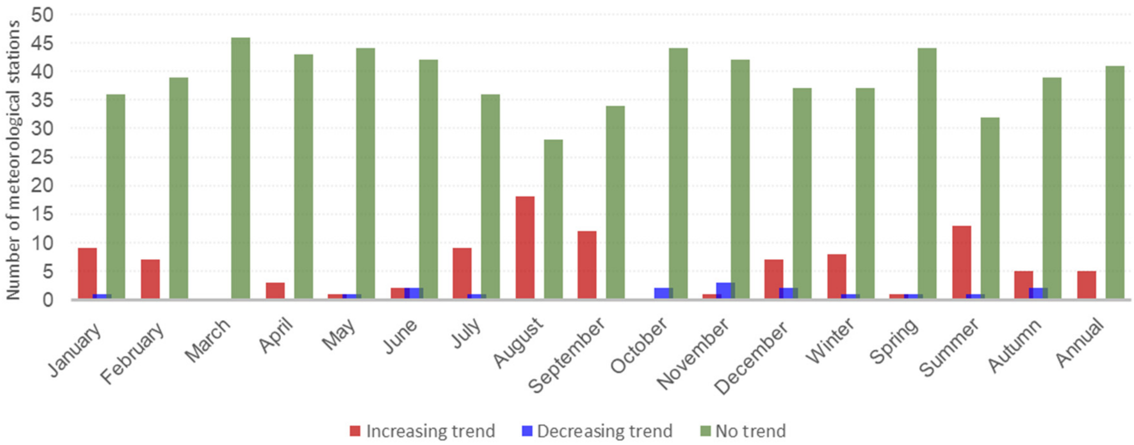

Figure 3. Summary of the trend of PET at different temporal scales.

3.2. Sen's Slope (the PET Trend Magnitude)

The magnitude of the PET trend in all 46 meteorological stations was also investigated. The results show that there were different magnitudes of the PET trend in different meteorological stations. On one side, the highest increase in the PET trend is recorded at the annual temporal scale for three stations located at the northern and eastern Sicilian coastline, namely, stations 228, 258, and 261 with 10.68 mm, 5.15 mm, and 4.96 mm per year, respectively. On the other side, the highest decrease in the PET trend is recorded for the meteorological station 231, situated on the western side of Mt. Etna, in both summer at a seasonal monthly temporal scale (3.28 mm) and July at a monthly temporal scale (1.82 mm). Additionally, the spring seasonal trend of station 230, another meteorological station located at foot of Mt. Etna, showed the third-highest decreasing trend with 1.67 mm in the last 21 years (Table 3).

Table 3. Sen's slope result in mm.

Code	Name	Jan	Feb	Mar	Apr	May	Jun	Jul	Aug	Sep	Oct	Nov	Dec	Winter	Spring	Summer	Autumn	Year
203	Aragona													0.63				
209	Licata	0.64						1.35	1.59					2.07				
212	Ribera						0.53	1.01	1.19	0.61								
214	Caltanissetta																	
215	Delia																	
218	Mazzarino	0.36								0.8						2.47	1.44	
219	Mussomeli								1.33				0.57					
224	Bronte	0.34			0.7				0.87							1.89		
227	Caltagirone		0.37										0.26	0.85				3.36
228	Catania		0.8														2.11	10.68
229	Riposto		0.54															
230	Linguaglossa					−1.37							0.63		−1.67			
231	Maletto						−1.24	−1.82								−3.28		
232	Mazzarrone								0.74					1.19				
233	Mineo					0.88	0.86	1.33	1.12	0.84			0.24	0.51		3.13		
234	Paternò									0.73		0.39					1.45	
235	Pedara										−0.62						−1.11	
237	Randazzo																	
238	Enna								1.58							3.42		
241	Nicosia				0.84					0.74								
249	S. P. Niceto																	
254	Naso						−0.62											
256	N. di Sicilia																	
258	Pettineo	0.72	0.62					0.67	1.04					1.75		2.14		5.15
261	Torregrotta							0.6	1.02	0.82						1.79	1.01	4.96
262	Alia				0.98							−0.5		1.01				
264	Camporeale	0.28								0.61			0.43					
265	Castelbuono	0.48																
269	Gangi								1.73	0.88								
273	Mezzojuso												−0.47				−1.51	
274	Misilmeri							0.66	0.78							1.53		
276	Palermo	0.61	0.79						0.8						1.41	1.69		
277	Partinico	0.56	0.68						1.27	0.82			0.44			2.77	1.73	
279	P. Generosa																	
222	Sclafani Bagni		0.6						1.43							2.46		
281	Termini Imerese							0.75								2.19		
282	Acate										−0.49							
283	Comiso							0.96	1.24							2.53		
286	Ragusa																	
287	S. C. Camerina	−0.41							0.77			−0.37	−0.39	−0.83				
288	Scicli																	
289	Augusta									0.45								
291	Francofonte									0.82			0.48	1.6		2.78		6.45
301	C. del Golfo											−0.3						
302	Castelvetrano	0.48						0.67	1.04	0.62								
305	Mazara del Vallo								1.33									
Max		0.72	0.8		0.98	0.88	0.86	1.35	1.73	0.88	−0.49	0.39	0.63	2.07	1.41	3.42	2.11	10.68
Min		−0.41	0.37		0.7	−1.37	−1.24	−1.82	0.74	0.45	−0.62	−0.5	−0.47	−0.83	−1.67	−3.28	−1.51	3.36
Average		0.36	0.62		0.84	−0.25	−0.14	0.47	1.17	0.72	−0.56	−0.15	0.21	0.91	−0.13	1.73	0.64	6.38

3.3. Spatial Distribution of the PET Trend

In order to further provide a detailed framework, a spatial distribution analysis on PET trends was also carried out. Therefore, the monthly, seasonal, and annual trends of PET in Sicily, over the last 21 years, were represented using GIS application, and then reported in Figure 4.

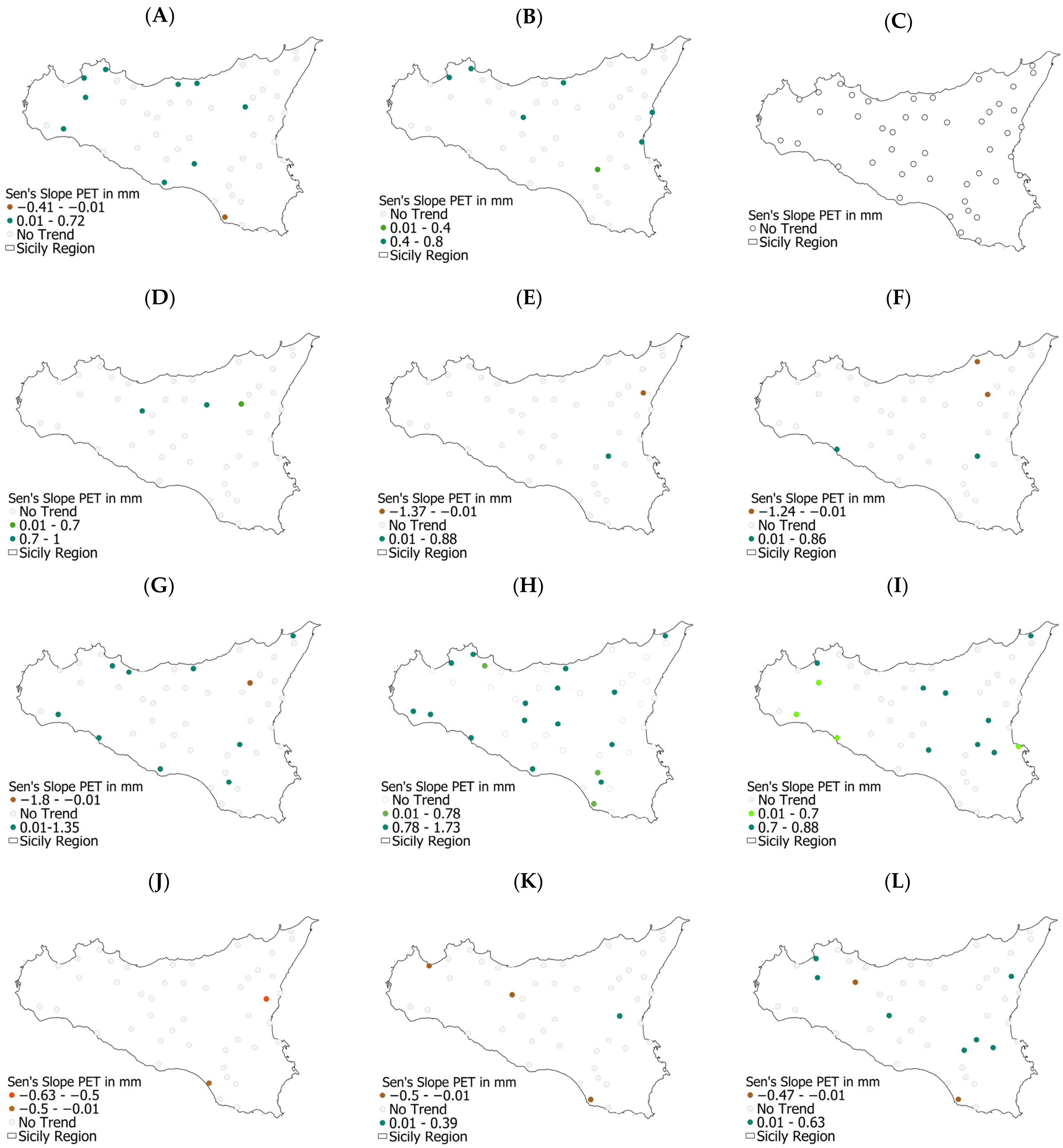

Figure 4. *Cont.*

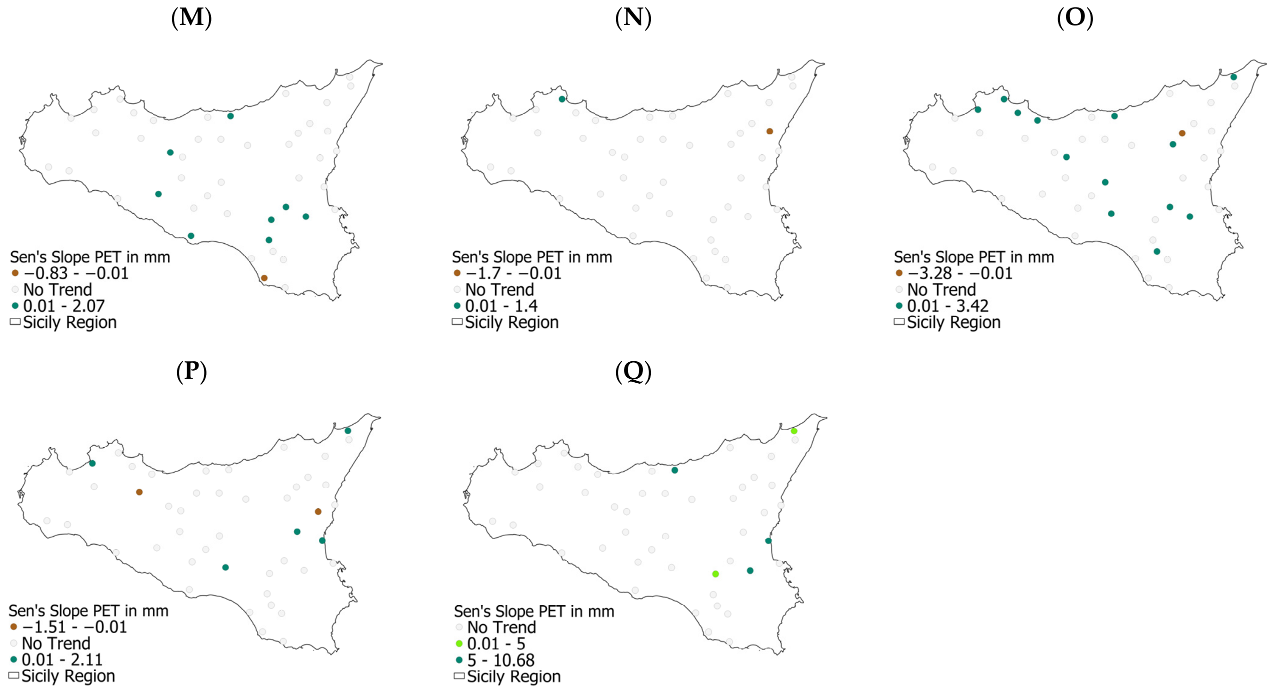

Figure 4. Map of the spatial distribution of the PET trend over Sicily in January (**A**), February (**B**), March (**C**), April (**D**), May (**E**), June (**F**), July (**G**), August (**H**), September (**I**), October (**J**), November (**K**), December (**L**), winter (**M**), spring (**N**), summer (**O**), autumn (**P**), and annually (**Q**).

3.4. Monthly Spatial Trend

Overall, the spatial distribution of PET trends, either positive or negative, does not highlight a specific tendency. Looking at the distributions from January to June at a monthly temporal scale, indeed, increasing trends of PET are prevalent, and involve a maximum of nine meteorological stations distributed fairly evenly within the island (January) and a minimum of one meteorological station (May). Furthermore, it should be noted that in March at the monthly scale, there is no trend, as previously noted. Going more into the details, (i) in January at the monthly scale, nine stations are of interest due to an increasing PET trend (Figure 4A) ranging between 0.72 mm and 0.28 mm, and only one station in the southern island shows a decreasing trend equal to 0.41 mm; (ii) in February at the monthly scale (Figure 4B), only increasing trends of PET are identified in seven meteorological stations distributed in the northern and eastern sides of Sicily; (iii) in April at the monthly scale (Figure 4D), just three meteorological stations are characterized by a PET trend, namely, an increasing trend ranging from 0.7 mm to 0.98 mm; (iv) in May at the monthly scale (Figure 4E), only one station presents an increasing trend (0.88 mm), and only another one presents a decreasing trend (1.37 mm), both stations placed in the eastern side of Sicily; (v) in June at the monthly scale (Figure 4F), four meteorological stations present a PET trend, specifically, two of them in the north-east with a decreasing trend (1.24 mm and 0.62 mm), whereas the other two in the centre of the island present an increasing trend (0.53 mm and 0.86 mm).

If the spatial trends' distribution is analysed in July, August, and September at the monthly scale, a general rise in the meteorological stations having PET trends may be observed. More specifically, with the exception of station 231 characterized by the second highest decreasing trend in July at the monthly scale (Figure 4G), all of the remaining present increasing PET trends range from 0.6 mm and 1.73 mm and are distributed within the surroundings of the coastlines, for the most part. Particular attention should be paid to August at the monthly scale, at which, increasing PET trends are detected in 18 meteorological stations (39%) distributed all over the region.

Finally, moving from October to December at the monthly scale, a general decrease in meteorological stations presenting PET trends can be observed. Specifically, (i) in October at the monthly scale (Figure 4J), only two meteorological stations located on the eastern and southern sides of Sicily, respectively, detected trends which were both decreasing (0.62 mm and 0.49 mm); (ii) in November at the monthly scale (Figure 4K), of the four meteorological stations involved in the trends, three of them, distributed from the north-west to the south of the island, present decreasing trends (0.5 mm, 0.37 mm, 0.3 mm), whereas only one station on the eastern side is characterized by an increasing PET trend (0.93 mm); (iii) in December at the monthly scale (Figure 4L), seven meteorological stations, scattered throughout the island, detected increasing trends of PET ranging from 0.24 mm to 0.57 mm, whereas two other stations on the north-west and south of the island detected decreasing trends of PET with 0.47 and 0.39 mm.

The stacked bar chart reported in Figure 5 summarizes, for each meteorological station and for each monthly scale, the magnitude of the detected PET trends. As can be seen, station 233, which is located on the south-eastern side of Sicily, recorded the highest number of PET trends (i.e., all increasing trends ranging from 2.11 mm to 2.95 mm) at the monthly scale, namely, from June to September, and December.

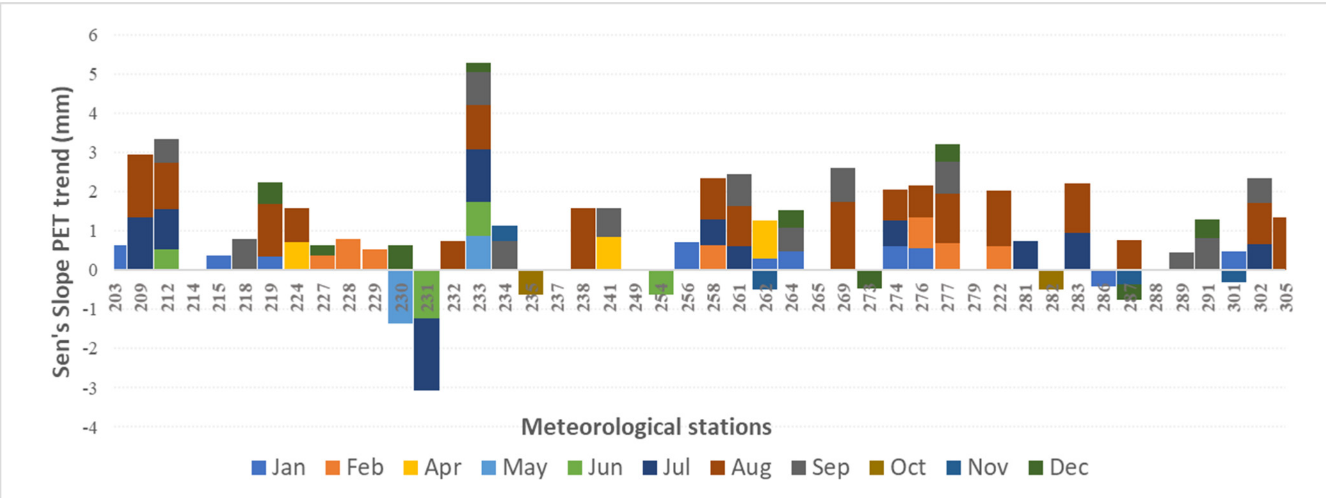

Figure 5. The monthly trend Sen's slope magnitude of PET in mm in all analysed meteorological stations.

3.5. Seasonal and Annual Spatial Trend

As previously mentioned, the spatial distribution analysis of PET trends was also carried out at the seasonal scale (Figure 4M–P) and at the annual scale (Figure 4Q). The results highlighted that in summer at the seasonal scale, among 14 meteorological stations involved in increasing PET trends ranging from 1.53 mm to 3.42 mm, only station 231 detected a decreasing trend, with the highest recorded value equal to 3.28 mm. On the contrary, in spring at the seasonal scale, only two meteorological stations in the north of the region highlighted PET trends, namely, an increasing (1.41 mm) one, and a decreasing one (1.67 mm). Regarding instead winter and autumn at the seasonal scale, nine and seven meteorological stations, respectively, detected PET trends with no specific spatial distribution within the island.

Lastly, at the annual scale, only five meteorological stations were analysed, located from the north-eastern side of Sicily to the eastern coast. They are characterized by increasing trends of PET, ranging from 3.36 mm (station 227) to 10.68 mm (station 228), which represents the highest trend in the region in the last 21 years. The stacked bar chart reported in Figure 6 summarizes, for each meteorological station and for each seasonal and annual scale, the magnitude of the detected PET trends.

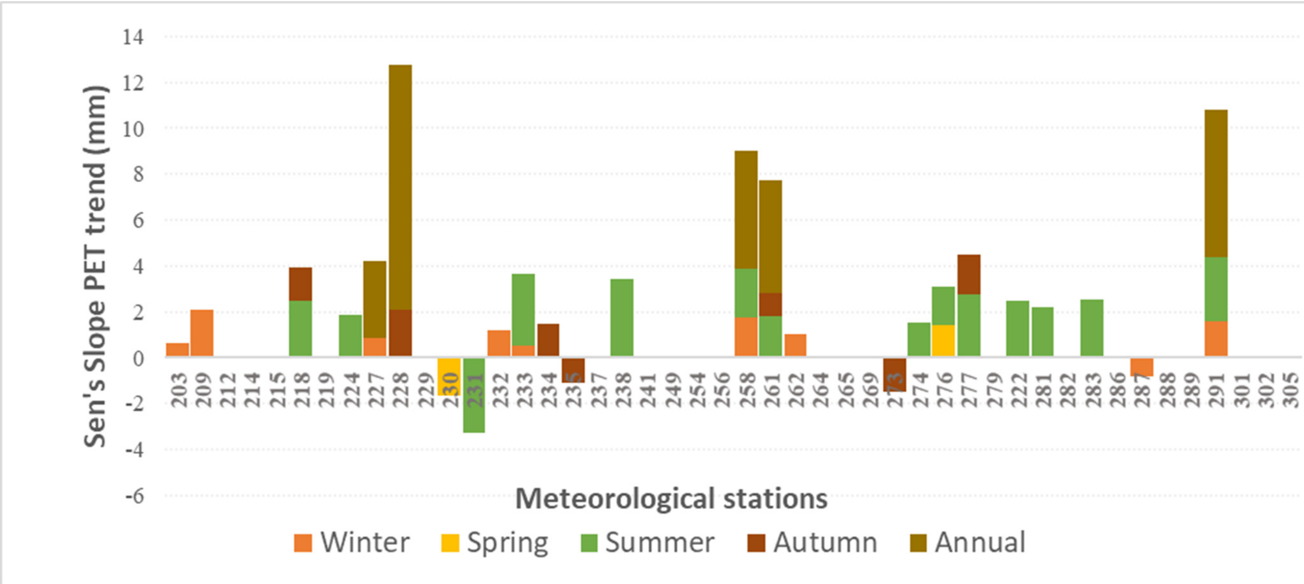

Figure 6. The seasonal and annual trend Sen's slope magnitude of PET in mm in different meteorological stations.

4. Discussion

The Temporal Trend of PET

As revealed in the literature, the analysis of PET trends was carried out for several other regions belonging to and distributed throughout Italy. Therefore, the results of our study were compared with those obtained for other regions inside Italy. In northern Italy, for instance, an increase in PET was observed in the upper part of the Adda river catchment in the Central Italian Alps [58,59]; in central Italy, an increasing trend of reference evapotranspiration from 1951 to 2008 [60] was also detected, with a specific reference to the Spoleto meteorological station, which showed an increasing annual trend of PET through the Hargreaves and Samini estimation model [61], and the historical meteorological station of the University of Bologna which highlighted an increase at all seasonal mean PETs (for the 1972–2007 period), with an increase of 13 mm in winter, 39 mm in spring, 60 mm in summer, and 14 mm in autumn [60]. Coming to southern Italy, increases in PET related to increasing temperatures [28] were observed. In more detail, the Apulia region is characterized by an annual PET trend equal to 18.6 mm [62], and particularly for the Apulian Tavoliere, an increasing trend of evapotranspiration of 8 mm per decade in 1957–2008 is recorded.

Beyond Italy, different parts of the world showed an increasing annual PET trend. The IPCC's sixth technical report, indeed, showed that there is an increase in evapotranspiration due to growing atmospheric water demand, which will decrease soil moisture over the Mediterranean region [1]. In more detail, the Mediterranean and Iberian regions showed increasing trends of evapotranspiration from 1971 to 2015 [63]. This is also confirmed by the recourse of different satellite sources through which it was possible to detect increasing evapotranspiration trends in several Mediterranean regions, including Sicily, from 2009 to 2018 [57]. Moving forward, in Spain, from 1922 to 2020, the evapotranspiration trend showed an increasing trend and resulted in the worsening of the growth of crop water requirements [64], as well as in the semi-arid part of Spain which presented an increasing annual trend from 1970 to 2000 and confirmed that the future projections indicate an increase [65]. Surprisingly, a monthly study revealed that June, the month with the biggest relative changes, is primarily responsible for guiding summer trends and spring trends, respectively [66]. That study's findings are likewise in line with ours, according to which, the majority of meteorological stations saw an upward trend over the spring and summer seasons (Figure 3). Moving out onto a broader view, an increase in the annual (0.009–0.026 mm/year) and seasonal (0.014–0.027 mm/year during southwest monsoon and 0.015–0.074 during northeast monsoon) ETo in peninsular Malaysia [67] was observed, as well as in most parts of the Wei River basin (WRB) [7], north-eastern China, the southern coastal region of China, the north-western corner of China [68], 90% of Moldova from 1981 to 2012 [69], South Korea [56], and the central and southern parts of Mongolia [70].

Concluding, if the evapotranspiration paradox is taken into account [12,28,53,67,71], our study on Sicily shows that it was observed as monthly and winter, spring, summer, and autumn seasonal trends in our study (Table 2). Similarly, in the Calabria region, an analysis carried out using the Hargreaves and Samani estimation model for PET showed a decreasing trend in the different winter, spring, summer, and autumn seasons and dry and wet seasons [72]. In south-eastern Umbria, Central Italy, in two areas, asymmetric warming results in a decreasing evapotranspiration level [61]. Moreover, our study confirmed that there was a decreasing trend of PET in January, May, June, July, October, November, and December. Likewise, the Calabria meteorological station analysis showed decreasing trend in all months [72].

5. Conclusions

Understanding trends of evapotranspiration is crucial for water resource management, irrigation, and the implementation of climate change adaptation measures. This study aimed at analysing trends of PET in Sicily (southern Italy) over the last 21 years using the hydro-meteorological data provided by 46 meteorological stations distributed all over the region. PET has been estimated by the FAO Penman–Monteith method, and the Mann–Kendall test as well as Sen's Slope estimator were used to identify the trends over time. The result showed that there were significant monthly, seasonal, and annual trends in different stations. August is the month where the majority of temporal trends were detected (18 out of 46 stations). On the other hand, for March, no trend was detected. Regarding the seasonal temporal scale, the summer season showed the highest number of stations with significant trends (14 stations), and the winter season was the one with the lowest number of significant trends (only 2 stations). For five locations, an increasing trend has been identified at the annual time scale. August corresponds to the highest increasing PET trend with 1.73 mm per year at one meteorological station. Regarding the seasonal temporal trend, meteorological station 238 had the highest increasing trend, with 3.42 mm/year in the summer season. Finally, the highest estimated increasing trend of annual PET is 10.68 mm/year. Overall, the analysis showed that there is an increasing trend in some parts of Sicily. This is key information for future agricultural irrigation practices and a call for the implementation of climate change adaptation measures. As a further development of this study, geostatistical techniques will be applied to spatialize the information derived for single locations.

Author Contributions: Conceptualization, T.M.A.; Formal Analysis, T.M.A., N.P. and D.J.P.; Funding Acquisition, G.S. and A.C.; Investigation, T.M.A.; Methodology, T.M.A.; Project Administration, G.S. and A.C.; Resources, G.S. and A.C.; Software, T.M.A.; Supervision, D.J.P., N.P. and A.C.; Validation, D.J.P. and N.P.; Visualization, T.M.A., N.P. and D.J.P.; Writing—original draft, T.M.A., N.P. and D.J.P.; writing/review and editing, T.M.A., D.J.P. and N.P. All authors have read and agreed to the published version of the manuscript.

Funding: This research was funded by Ambiens S.r.l through a grant with University of Catania signed on 23 July 2020, and it was partially carried out within the project HydrEx—Hydrological extremes in a changing climate-Piano di incentivi per la ricerca di Ateneo (Pia.ce.ri.), 2020–2022, Università di Catania. Nunziarita Palazzolo is supported by post-doctoral contract "Eventi idrologici estremi e resilienza ai cambiamenti climatici", funded within the activities of the research project "LIFE SimetoRES–Urban adaption and community learning for a RESilient Simeto Valley"-grant agreement no. LIFE17CCA/IT/000115–CUP C65H18000550006.

Data Availability Statement: Due to the large size of the database, the data reported in this study are available upon request.

Acknowledgments: The authors would like to thank the SIAS service that provided 21 years of meteorological data.

Conflicts of Interest: The authors declare that they have no known competing financial interests or personal relationships that could have appeared to influence the work reported in this paper.

References

1. IPCC. *Climate Change 2021: The Physical Science Basis. Contribution of Working Group I to the Sixth Assessment Report of the Intergovernmental Panel on Climate Change*; Masson-Delmotte, V., Zhai, P., Pirani, A., Connors, S.L., Péan, C., Berger, S., Caud, N., Chen, Y., Goldfarb, L., Gomis, M.I., et al., Eds.; Cambridge University Press: Cambridge, UK; New York, NY, USA, 2021; 2391p.
2. Fischer, E.M.; Sippel, S.; Knutti, R. Increasing Probability of Record-Shattering Climate Extremes. *Nat. Clim. Chang.* **2021**, *11*, 689–695. [CrossRef]
3. IPCC. *2018: Global Warming of 1.5 °C. An IPCC Special Report on the Impacts of Global Warming of 1.5 °C above Pre-Industrial Levels and Related Global Greenhouse Gas Emission Pathways, in the Context of Strengthening the Global Response to the Threat of Climate Change, Sustainable Development, and Efforts to Eradicate Poverty*; Masson-Delmotte, V., Zhai, P., Pörtner, H.-O., Roberts, D., Skea, J., Shukla, P.R., Pirani, A., Moufouma-Okia, W., Péan, C., Pidcock, R., et al., Eds.; Cambridge University Press: Cambridge, UK; New York, NY, USA, 2018; 616p. [CrossRef]
4. Huang, H.; Han, Y.; Cao, M.; Song, J.; Xiao, H.; Cheng, W. Spatiotemporal Characteristics of Evapotranspiration Paradox and Impact Factors in China in the Period of 1960–2013. *Adv. Meteorol.* **2015**, *2015*, 519207. [CrossRef]
5. Wang, Z.; Xie, P.; Lai, C.; Chen, X.; Wu, X.; Zeng, Z.; Li, J. Spatiotemporal Variability of Reference Evapotranspiration and Contributing Climatic Factors in China during 1961–2013. *J. Hydrol.* **2017**, *544*, 97–108. [CrossRef]
6. Liu, Q.; Yan, C.; Ju, H.; Garré, S. Impact of Climate Change on Potential Evapotranspiration under a Historical and Future Climate Scenario in the Huang-Huai-Hai Plain, China. *Theor. Appl. Climatol.* **2018**, *132*, 387–401. [CrossRef]
7. Zuo, D.; Xu, Z.; Yang, H.; Liu, X. Spatiotemporal Variations and Abrupt Changes of Potential Evapotranspiration and Its Sensitivity to Key Meteorological Variables in the Wei River Basin, China. *Hydrol. Process.* **2012**, *26*, 1149–1160. [CrossRef]
8. Bian, Y.; Dai, H.; Zhang, Q.; Yang, L.; Du, W. Spatial Distribution of Potential Evapotranspiration Trends in the Inner Mongolia Autonomous Region (1971–2016). *Theor. Appl. Climatol.* **2020**, *140*, 1161–1169. [CrossRef]
9. Ding, Y.; Peng, S. Spatiotemporal Change and Attribution of Potential Evapotranspiration over China from 1901 to 2100. *Theor. Appl. Climatol.* **2021**, *145*, 79–94. [CrossRef]
10. Zongxing, L.; Qi, F.; Wei, L.; Tingting, W.; Yan, G.; Yamin, W.; Aifang, C.; Jianguo, L.; Li, L. Spatial and Temporal Trend of Potential Evapotranspiration and Related Driving Forces in Southwestern China, during 1961–2009. *Quat. Int.* **2014**, *336*, 127–144. [CrossRef]
11. Han, X.; Liu, W.; Lin, W. Spatiotemporal Analysis of Potential Evapotranspiration in the Changwu Tableland from 1957 to 2012. *Meteorol. App.* **2015**, *591*, 586–591. [CrossRef]
12. Zhao, Y.; Zou, X.; Cao, L.; Yao, Y.; Fu, G. Spatiotemporal Variations of Potential Evapotranspiration and Aridity Index in Relation to Influencing Factors over Southwest China during 1960–2013. *Theor. Appl. Climatol.* **2018**, *133*, 711–726. [CrossRef]
13. Guo, Q.; Liang, J.; Cao, X.; Zhang, Z.; Zhang, L. Spatiotemporal Evolution of Evapotranspiration in China after 1998. *Water* **2020**, *12*, 3250. [CrossRef]
14. Maruyama, A.; Ohba, K.; Kurose, Y.; Miyamoto, T. Seasonal Variation in Evapotranspiration from Mat Rush Grown in Paddy Field. *J. Agric. Meteorol.* **2004**, *60*, 1–15. [CrossRef]
15. Li, X.; Gemmer, M.; Zhai, J.; Liu, X.; Su, B.; Wang, Y. Spatio-Temporal Variation of Actual Evapotranspiration in the Haihe River Basin of the Past 50 Years. *Quat. Int.* **2013**, *304*, 133–141. [CrossRef]
16. Chu, R.; Li, M.; Islam, A.R.M.T.; Fei, D.; Shen, S. Attribution Analysis of Actual and Potential Evapotranspiration Changes Based on the Complementary Relationship Theory in the Huai River Basin of Eastern China. *Int. J. Climatol.* **2019**, *39*, 4072–4090. [CrossRef]
17. Shadmani, M.; Marofi, S.; Roknian, M. Trend Analysis in Reference Evapotranspiration Using Mann-Kendall and Spearman's Rho Tests in Arid Regions of Iran. *Water Resour. Manag.* **2012**, *26*, 211–224. [CrossRef]
18. Luo, Y.; Gao, P.; Mu, X. Influence of Meteorological Factors on the Potential Evapotranspiration in Yanhe River Basin, China. *Water* **2021**, *13*, 1222. [CrossRef]
19. Jerin, J.N.; Islam, H.M.T.; Islam, A.R.M.T.; Shahid, S.; Hu, Z.; Badhan, M.A.; Chu, R.; Elbeltagi, A. Spatiotemporal Trends in Reference Evapotranspiration and Its Driving Factors in Bangladesh. *Theor. Appl. Climatol.* **2021**, *144*, 793–808. [CrossRef]
20. Ndiaye, P.M.; Bodian, A.; Diop, L.; Deme, A.; Dezetter, A.; Djaman, K.; Ogilvie, A. Trend and Sensitivity Analysis of Reference Evapotranspiration in the Senegal River Basin Using NASA Meteorological Data. *Water* **2020**, *12*, 1957. [CrossRef]
21. Palumbo, A.D.; Vitale, D.; Campi, P.; Mastrorilli, M. Time Trend in Reference Evapotranspiration: Analysis of a Long Series of Agrometeorological Measurements in Southern Italy. *Irrig. Drain. Syst.* **2011**, *25*, 395–411. [CrossRef]
22. Maček, U.; Bezak, N.; Šraj, M. Reference Evapotranspiration Changes in Slovenia, Europe. *Agric. For. Meteorol.* **2018**, *260–261*, 183–192. [CrossRef]

23. Chaouche, K.; Neppel, L.; Dieulin, C.; Pujol, N.; Ladouche, B.; Martin, E.; Salas, D.; Caballero, Y. Analyses of Precipitation, Temperature and Evapotranspiration in a French Mediterranean Region in the Context of Climate Change. *Comptes Rendus-Geosci.* **2010**, *342*, 234–243. [CrossRef]
24. Wang, R.; Li, L.; Chen, L.; Ning, L.; Yuan, L.; Guonian, L. Respective Contributions of Precipitation and Potential Evapotranspiration to Long-Term Changes in Global Drought Duration and Intensity. *Int. J. Climatol.* **2022**, *42*, 10126–10137. [CrossRef]
25. Aieb, A.; Kadri, I.; Lefsih, K.; Madani, K. Spatiotemporal Trend Analysis of Runoff and Actual Evapotranspiration in Northern Algeria between 1901 and 2020. *Model. Earth Syst. Environ.* **2022**, *8*, 5251–5267. [CrossRef]
26. Zeng, J.; Li, J.; Lu, X.; Wei, Z.; Shangguan, W.; Zhang, S.; Dai, Y.; Zhang, S. Assessment of Global Meteorological, Hydrological and Agricultural Drought under Future Warming Based on CMIP6. *Atmos. Ocean. Sci. Lett.* **2022**, *15*, 100143. [CrossRef]
27. Stefanidis, S.; Alexandridis, V. Precipitation and Potential Evapotranspiration Temporal Variability and Their Relationship in Two Forest Ecosystems in Greece. *Hydrology* **2021**, *8*, 160. [CrossRef]
28. Liuzzo, L.; Viola, F.; Noto, L.V. Wind Speed and Temperature Trends Impacts on Reference Evapotranspiration in Southern Italy. *Theor. Appl. Climatol.* **2016**, *123*, 43–62. [CrossRef]
29. Peres, D.J.; Modica, R.; Cancelliere, A. Assessing Future Impacts of Climate Change on Water Supply System Performance: Application to the Pozzillo Reservoir in Sicily, Italy. *Water* **2019**, *11*, 2531. [CrossRef]
30. Torina, A.; Khoury, C. Ticks Infesting Livestock on Farms in Western Sicily, Italy. *Experimental Appl. Acarol.* **2006**, *38*, 75–86. [CrossRef]
31. Bonaccorso, B.; Cancelliere, A.; Rossi, G. Probabilistic Forecasting of Drought Class Transitions in Sicily (Italy) Using Standardized Precipitation Index and North Atlantic Oscillation Index. *J. Hydrol.* **2015**, *526*, 136–150. [CrossRef]
32. Lang, D.; Zheng, J.; Shi, J.; Liao, F.; Ma, X.; Wang, W.; Chen, X.; Zhang, M. A Comparative Study of Potential Evapotranspiration Estimation by Eight Methods with FAO Penman–Monteith Method in Southwestern China. *Water* **2017**, *9*, 734. [CrossRef]
33. Ndulue, E.; Ranjan, R.S. Performance of the FAO Penman-Monteith Equation under Limiting Conditions and Fourteen Reference Evapotranspiration Models in Southern Manitoba. *Theor. Appl. Climatol.* **2021**, *143*, 1285–1298. [CrossRef]
34. Utset, A.; Farré, I.; Martínez-Cob, A.; Cavero, J. Comparing Penman-Monteith and Priestley-Taylor Approaches as Reference-Evapotranspiration Inputs for Modeling Maize Water-Use under Mediterranean Conditions. *Agric. Water Manag.* **2004**, *66*, 205–219. [CrossRef]
35. Shi, T.T.; Guan, D.X.; Wu, J.B.; Wang, A.Z.; Jin, C.J.; Han, S.J. Comparison of Methods for Estimating Evapotranspiration Rate of Dry Forest Canopy: Eddy Covariance, Bowen Ratio Energy Balance, and Penman-Monteith Equation. *J. Geophys. Res. Atmos.* **2008**, *113*, 1–15. [CrossRef]
36. Tellen, V.A. A Comparative Analysis of Reference Evapotranspiration from the Surface of Rainfed Grass in Yaounde, Calculated by Six Empirical Methods against the Penman-Monteith Formula. *Earth Perspect.* **2017**, *4*, 17–28. [CrossRef]
37. Peng, L.; Li, Y.; Feng, H. The Best Alternative for Estimating Reference Crop Evapotranspiration in Different Sub-Regions of Mainland China. *Sci. Rep.* **2017**, *7*, 1–19. [CrossRef] [PubMed]
38. Alemu, H.; Kaptué, A.T.; Senay, G.B.; Wimberly, M.C.; Henebry, G.M. Evapotranspiration in the Nile Basin: Identifying Dynamics and Drivers, 2002–2011. *Water* **2015**, *7*, 4914–4931. [CrossRef]
39. Aschale, T.M.; Peres, D.J.; Gullotta, A.; Sciuto, G.; Cancelliere, A. Trend Analysis and Identification of the Meteorological Factors Influencing Reference Evapotranspiration. *Water* **2023**, *15*, 470. [CrossRef]
40. Dong, Q.; Ding, Y.; Fu, J. The Response of Reference Evapotranspiration to Climate Change in Xinjiang, China: Historical Changes, Driving Forces, and Future Projections. *Int. J. Climtol.* **2020**, *40*, 235–254. [CrossRef]
41. He, D.; Liu, Y.; Pan, Z.; An, P.; Wang, L.; Dong, Z. Climate Change and Its Effect on Reference Crop Evapotranspiration in Central and Western Inner Mongolia during 1961–2009. *Int. J. Climatol.* **2013**, *7*, 417–428. [CrossRef]
42. Hui-mean, F.; Yusof, F. Drought Analysis and Water Resource Availability Using Standardised Precipitation Evapotranspiration Index. *Atmos. Res.* **2018**, *201*, 102–115. [CrossRef]
43. Nam, W.; Hong, E.; Choi, J. Has Climate Change Already Affected the Spatial Distribution and Temporal Trends of Reference Evapotranspiration in South Korea ? *Agric. Water Manag.* **2015**, *150*, 129–138. [CrossRef]
44. Peng, S.; Ding, Y.; Wen, Z.; Chen, Y.; Cao, Y.; Ren, J. Spatiotemporal Change and Trend Analysis of Potential Evapotranspiration over the Loess Plateau of China during 2011–2100. *Agric. For. Meteorol.* **2017**, *233*, 183–194. [CrossRef]
45. Diop, L.; Bodian, A.; Diallo, D. Spatiotemporal Trend Analysis of the Mean Annual Rainfall in Senegal. *Eur. Sci. J. ESJ* **2016**, *12*, 231. [CrossRef]
46. Wu, H.; Xu, M.; Peng, Z.; Chen, X. Temporal Variations in Reference Evapotranspiration in the Tarim River Basin, Central Asia. *PLoS ONE* **2021**, *16*, 1–17. [CrossRef]
47. Zhang, F.; Geng, M.; Wu, Q.; Liang, Y. Study on the Spatial-Temporal Variation in Evapotranspiration in China from 1948 to 2018. *Sci. Rep.* **2020**, 1–13. [CrossRef]
48. Ahmad, I.; Tang, D.; Wang, T.; Wang, M.; Wagan, B. Precipitation Trends over Time Using Mann-Kendall and Spearman's Rho Tests in Swat River Basin, Pakistan. *Adv. Meteorol.* **2015**, *2015*, 431860. [CrossRef]
49. Darshana; Pandey, A.; Pandey, R.P. Analysing Trends in Reference Evapotranspiration and Weather Variables in the Tons River Basin in Central India. *Stoch. Environ. Res. Risk Assess.* **2013**, *27*, 1407–1421. [CrossRef]
50. Kamal, N. Mann-Kendall, and Sen's Slope Estimators for Precipitation Trend Analysis in North-Eastern States of India. *IJCA* **2019**, *177*, 7–16. [CrossRef]

51. Panda, A.; Sahu, N. Trend Analysis of Seasonal Rainfall and Temperature Pattern in Kalahandi, Bolangir and Koraput Districts of Odisha, India. *Atmos. Sci. Lett.* **2019**, *20*, 1002. [CrossRef]
52. Peng, Z.; Stovin, V. Independent Validation of the SWMM Green Roof Module. *J. Hydrol. Eng.* **2017**, *22*, 1–12. [CrossRef]
53. Shan, N.; Shi, Z.; Yang, X.; Gao, J.; Cai, D. Spatiotemporal Trends of Reference Evapotranspiration and Its Driving Factors in the Beijing-Tianjin Sand Source Control Project Region, China. *Agric. For. Meteorol.* **2015**, *200*, 322–333. [CrossRef]
54. Eymen, A.; Köylü, Ü. Seasonal Trend Analysis and ARIMA Modeling of Relative Humidity and Wind Speed Time Series around Yamula Dam. *Meteorol. Atmos. Phys.* **2019**, *131*, 601–612. [CrossRef]
55. Hu, M.; Sayama, T.; Try, S.; Takara, K.; Tanaka, K. Trend Analysis of Hydroclimatic Variables in the Kamo River Basin, Japan. *Water* **2019**, *11*, 1782. [CrossRef]
56. Hwang, J.H.; Azam, M.; Jin, M.S.; Kang, Y.H.; Lee, J.E.; Latif, M.; Ahmed, R.; Umar, M.; Hashmi, M.Z. Spatiotemporal Trends in Reference Evapotranspiration over South Korea. *Paddy Water Environ.* **2020**, *18*, 235–259. [CrossRef]
57. Li, W.; Perera, S.; Linstead, E.; Thomas, R.; El-Askary, H.; Piechota, T.; Struppa, D. Investigating Decadal Changes of Multiple Hydrological Products and Land-Cover Changes in the Mediterranean Region for 2009–2018. *Earth Syst. Environ.* **2021**, *5*, 285–302. [CrossRef]
58. Crespi, A.; Brunetti, M.; Ranzi, R.; Tomirotti, M.; Maugeri, M. A Multi-Century Meteo-Hydrological Analysis for the Adda River Basin (Central Alps). Part I: Gridded Monthly Precipitation (1800–2016) Records. *Int. J. Climatol.* **2021**, *41*, 162–180. [CrossRef]
59. Ranzi, R.; Michailidi, E.M.; Tomirotti, M.; Crespi, A.; Brunetti, M.; Maugeri, M. A Multi-Century Meteo-Hydrological Analysis for the Adda River Basin (Central Alps). Part II: Daily Runoff (1845–2016) at Different Scales. *Int. J. Climatol.* **2021**, *41*, 181–199. [CrossRef]
60. Vergni, L.; Todisco, F. Spatio-Temporal Variability of Precipitation, Temperature and Agricultural Drought Indices in Central Italy. *Agric. For. Meteorol.* **2011**, *151*, 301–313. [CrossRef]
61. Todisco, F.; Vergni, L. Climatic Changes in Central Italy and Their Potential Effects on Corn Water Consumption. *Agric. For. Meteorol.* **2008**, *148*, 1–11. [CrossRef]
62. Elferchichi, A.; Giorgio, G.A.; Lamaddalena, N.; Ragosta, M.; Telesca, V. Variability of Temperature and Its Impact on Reference Evapotranspiration: The Test Case of the Apulia Region (Southern Italy). *Sustainability* **2017**, *9*, 2337. [CrossRef]
63. Páscoa, P.; Russo, A.; Gouveia, C.M.; Soares, P.M.M.; Cardoso, R.M.; Careto, J.A.M.; Ribeiro, A.F.S. A High-Resolution View of the Recent Drought Trends over the Iberian Peninsula. *Weather Clim. Extrem.* **2021**, *32*, 100320. [CrossRef]
64. Vila-Traver, J.; Aguilera, E.; Infante-Amate, J.; González de Molina, M. Climate Change and Industrialization as the Main Drivers of Spanish Agriculture Water Stress. *Sci. Total Environ.* **2021**, *760*, 143399. [CrossRef] [PubMed]
65. Ruiz-ÁÍvarez, M.; Gomariz-Castillo, F.; Alonso-Sarría, F. Evapotranspiration Response to Climate Change in Semi-Arid Areas: Using Random Forest as Multi-Model Ensemble Method. *Water* **2021**, *13*, 222. [CrossRef]
66. Tomas-Burguera, M.; Beguería, S.; Vicente-Serrano, S.M. Climatology and Trends of Reference Evapotranspiration in Spain. *Int. J. Climatol.* **2021**, *41*, E1860–E1874. [CrossRef]
67. Hadi, S.; Khairi, A.; Wahab, A.; Shahid, S.; Bin, Z. Changes in Reference Evapotranspiration and Its Driving Factors in Peninsular Malaysia. *Atmos. Res.* **2020**, *246*, 105096. [CrossRef]
68. Yang, J.; Wang, W.; Hua, T.; Peng, M. Spatiotemporal Variation of Actual Evapotranspiration and Its Response to Changes of Major Meteorological Factors over China Using Multi-Source Data. *J. Water Clim. Chang.* **2021**, *12*, 325–338. [CrossRef]
69. Piticar, A.; Mihăilă, D.; Lazurca, L.G.; Bistricean, P.I.; Puţuntică, A.; Briciu, A.E. Spatiotemporal Distribution of Reference Evapotranspiration in the Republic of Moldova. *Theor. Appl. Climatol.* **2016**, *124*, 1133–1144. [CrossRef]
70. Yu, W.; Wu, T.; Wang, W.; Li, R.; Wang, T.; Qin, Y.; Wang, W.; Zhu, X. Spatiotemporal Changes of Reference Evapotranspiration in Mongolia during 1980–2006. *Adv. Meteorol.* **2016**, *2016*, 9586896. [CrossRef]
71. Vicente-Serrano, S.M.; Azorin-Molina, C.; Sanchez-Lorenzo, A.; Revuelto, J.; López-Moreno, J.I.; González-Hidalgo, J.C.; Moran-Tejeda, E.; Espejo, F. Reference Evapotranspiration Variability and Trends in Spain, 1961–2011. *Glob. Planet. Chang.* **2014**, *121*, 26–40. [CrossRef]
72. Capra, A.; Consoli, S.; Scicolone, B. Long-Term Climatic Variability in Calabria and Effects on Drought and Agrometeorological Parameters. *Water Resour. Manag.* **2013**, *27*, 601–617. [CrossRef]